Journal of Theoretical and Applied Physics (2020) 14:285–293
https://doi.org/10.1007/s40094-020-00382-5

RESEARCH

Microstrain and lattice disorder in nanocrystalline titanium dioxide prepared by chemical route and its relation with phase transformation

Apurba Kanti Deb[1] · **Partha Chatterjee**[2]

Received: 30 August 2019 / Accepted: 14 June 2020 / Published online: 23 June 2020

Abstract

The microstructure of nanocrystalline titanium dioxide (TiO_2), synthesized by chemical route, is studied from X-ray peak profile analysis and transmission electron microscopy. The broadening of the X-ray diffraction peaks indicates the presence of small crystallites with a significant amount of disorder. The progression of broadening at lower annealing temperatures, suggests the decrease in the strain broadening. The nano-TiO_2 was found to transform partially to rutile phase from its nanocrystalline anatase phase when annealed at a temperature of 750 °C. No further appreciable change was observed after annealing at higher temperature. The lattice parameters of the anatase phase change non-linearly with temperature. It was found that there is a discontinuous change in the value of crystallite size, microstrain and thermal parameter values accompanying with the phase transformation. The microstrain associated with the nanocrystalline grain is closely associated with thermal disorder and oxygen z-displacement. The value of thermal parameter reveals a significant deviation of the Ti atom from the regular lattice sites. The present study reveals that nanocrystalline anatase TiO_2 prepared by chemical route shows significant static disorder, which decreases with the increase in the annealing temperature along with concomitant phase transformation.

Keywords Nanocrystalline TiO_2 · X-ray powder diffraction · Phase transformation · Rietveld analysis · High-resolution transmission electron microscopy

Introduction

Nanotitanium dioxide (n-TiO_2) has been investigated in the recent years due to its electronic and optical properties. Titanium dioxide (TiO2) is of great interest due to several reasons such as good chemical stability, nontoxicity, optical transmittance and photo-induced properties [1–5]. This material is used in various applications such as photocatalytic decomposition of toxic compounds [5, 6], antibacterial and self-cleaning material [7, 8], in solar cells [9] or hydrogen generation from water and sunlight [10]. The desired properties of TiO2 are strongly influenced by phase composition, crystallinity, and/or microstructure.

✉ Apurba Kanti Deb
deb.apurba@gmail.com

[1] Department of Physics, Raiganj University, Raiganj, Uttar Dinajpur 733134, India

[2] Department of Physics, Vivekananda Mahavidyalaya, Haripal, Hooghly 712405, India

The rutile polymorph of TiO_2 having tetragonal symmetry with space group $P4_2/mnm$ is the most available phase of titanium dioxide due to its larger stability. The other two relatively less stable well-known phases are anatase and brookite with space group $I4_1/amd$ and $Pbca$, respectively, having tetragonal and orthorhombic crystal symmetries [11–13].

Nanocrystalline TiO_2 particles have been successfully synthesized by various techniques like gas condensation, solution phase synthesis [14, 15], combustion flame synthesis [16], chemical vapour deposition [17, 18] and sol–gel process [19, 20]. Apart from the above-mentioned chemical methods, physical deposition method like laser ablation has been utilized for the producing phase pureTiO_2 nanoparticles from pure Ti targets in water or other medium [21–23]. Experimental results showed that the microstructure, phase transformation kinetics and other related properties of nanocrystalline TiO_2 depends on the synthesis technique and the processing conditions. For example, large tensile stress in the thin films of titania can enhance its photo-induced hydrophilic behavior significantly [13]. The functional properties of TiO_2 are strongly dependent on

its phase and microstructure [24, 25]. The crystallite size is critical for phase stability, and the presence of micro- and/or macro-strains may affect the photo-induced hydrophilicity [26]. However, only a few reports investigated on the role of strain and size induced broadening of XRD peaks in TiO_2 NCs [27]. Tripathi et al. reported the temperature-dependent variation of strain in TiO_2 NCs [28]. The strain analysis has been mostly limited to Williamson–Hall (WH) method [29]. Several authors have studied the effect of stress and strain and is estimated by W–H analysis, uniform deformation model (UDM) and the modified form of W–H analysis namely uniform stress deformation model (USDM), uniform deformation energy density model (UDEDM) and size–strain plot (SSP) [30–32]. Rajender and Giri [31] studied the evaluation of lattice strain in ball milled TiO_2. They observed significant lattice strain in n-anatase particles of sizes of the order of 10 nm by both TEM and XRD analysis using a simplified WH analysis based on the above models. They attributed the origin of lattice microstrain to be dislocations. Seetharaman, and Dhanuskodi [32] performed size–strain analysis on the similar lines for n-TiO_2 synthesised by sol–gel route, but observed lower values for lattice strain. The results obtained, however, suffer from significant scatter in the WH plots. However, an extensive analysis of the X-ray diffraction (XRD) data by means of fitting of line shape with various models and/or Rietveld method has been limited [11, 33, 34]. Vives and Meunier [33] used both Williamson–Hall method and Rietveld method for the analysis of microstructure and observed that the rate of transformation of nanocrystalline a-TiO_2 prepared by sol–gel route to the rutile phase upon calcining is dependent on the microstructure and hence on the sol composition. They observed rapid increase in the crystallite size and hence a rapid rate of phase transformation to the rutile phase. However, an unambiguous value for the critical value of crystallite size for anatase to rutile phase transformation could not be predicted from the above studies [30–34].

At high temperatures, many nanophase ceramic materials undergo solid–solid phase transitions as they convert from metastable crystal structures to the stable thermodynamic phase. These transitions are of importance to powder ceramic processing as their occurrence can lead to large volume changes resulting in cracks or defects in dense sintered ceramics [35–37]. An important issue in the understanding of these processes is the role of the initial nanocrystal grain size on the temperature of the transition. In smaller particles, the greater surface area can have drastic effects on the thermodynamic stability as well as the kinetics of phase transformations.

The objective of the present work is to synthesize nanocrystalline TiO_2 by chemical process (sol–gel route) and to study the phase transformation behaviour with the annealing temperature. The study of phase transformation of anatase to rutile is of great importance from the application point of view, in particular for photocatalytic activity. Thus it is advantageous to improve or restrain the rate of transformation to have a specific phase or their mixture following the heat treatment [12]. Most of the studies reported so far [30–34] uses either simple Scherrer formula or Williamson–Hall method [29] or its variants which greatly undermines the values of crystallite size/microstrains due to the assumptions inherent in the method of analysis. A detailed simultaneous structural and microstructural investigation, using X-ray powder diffraction technique, is carried out in the present work using a modified Rietveld method and further corroborated using transmission electron microscopy. Attempts will be made in this communication to correlate the structural and microstructural parameter with the phase transformation and to elucidate the origin of lattice microstrain.

Experimental procedure

Nanocrystalline TiO_2 particles were prepared in the chemical method [38, 39]. For this, initially 1 ml of titanium isopropoxide was dissolved into 20 ml of 2-propanol. This solution was then slowly added with a syringe (5 ml) into 200 ml of H_2O containing 1.2 ml of concentrated HNO_3 in an ice bath. This addition was carried out in an inert atmosphere (N_2) and then stirred for about 4 h. The solvent was then removed using a rotary vacuum evaporator and dried in a vacuum desiccator. During the drying process, small amount of NaOH was kept inside the desiccator, which helps in removing the excess HNO_3. The resulting white powder was then characterized by X-ray powder diffraction and high-resolution transmission electron microscopy (HRTEM). The as-prepared specimen was subsequently annealed isothermally at different higher temperatures in air for 6 h to study the phase transformation properties.

The X-ray powder diffraction patterns of the as-prepared and annealed samples as well as the standard material (here fully recrystallized Si powder) [40] were taken at ambient temperature in a X'Pert PRO Diffractometer (PW 3040/60, PANanalytical) operating at 45 kV and 40 mA (slits system: Divergence/ Anti Scatter/ Receiving: 1°/1°/0.1 mm respectively), using Ni filtered CuK_α radiation. The data were collected in a step scan mode with a step size of 0.02° 2θ and the counting time of 10 s per step was chosen to get a good signal to noise ratio. The HRTEM micrographs were taken using a JEOL-TEM-2010 transmission electron microscope operating at 200 kV.

Results and discussion

Phase analysis

Figure 1 shows the X-ray diffraction pattern of the as-prepared n-TiO_2 and the same annealed at several temperatures. The as-prepared sample as well as the sample annealed at 100 °C is observed to be predominantly amorphous in nature and probably contain anatase TiO_2 (a-TiO_2) as the major component. The broadening of the X-ray diffraction peaks suggests that the a-TiO_2 crystallites are small and contains a significant amount of disorder due to reduced crystallinity. It can be argued from the crystallographic point of view that due to more flexible assembly of TiO_6 octahedra and a larger cell volume, the anatase phase is generally the principal crystalline phase formed in chemical synthesis routes [12]. However, for certain high-temperature applications, the performance of TiO_2-based devices may be modified/changed due to the phase transition [12]. Therefore, an understanding of the stabilities of these TiO_2 polymorphs is essential. It has already been reported that for photovoltaic applications, coexistence of both the rutile and the anatase phases in the material give better response [41–44]. Ohtani et al.[45] have shown that the brookite polymorph of TiO_2 does have the ability to show photocatalytic activity. However, we did not observe any brookite phase in the present method adopted by us.

Depending on the synthesis procedure and the starting chemicals used, the temperature for the anatase to rutile phase transition varies in a wide range. In air, this transition is reported to begin at around 600 °C [12]. There are several factors such as particle size and shape, surface area heating rate etc. which influences the phase transformation temperature as well as the kinetics. We have chosen higher temperature of upto 1000 °C to determine the phase transformation and phase composition of the resultant powders.

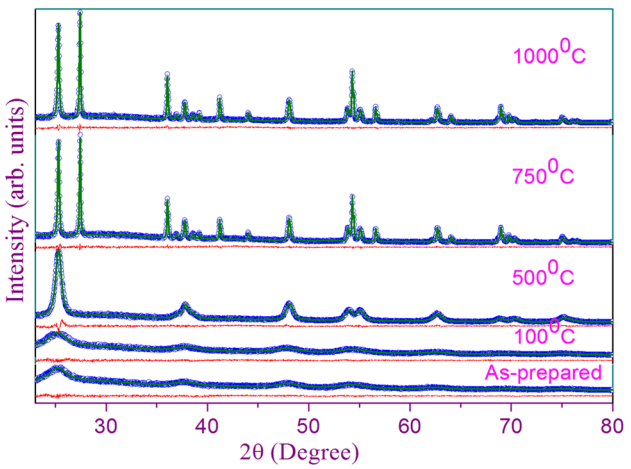

Fig. 1 Selected range X-ray powder diffraction pattern for the as-prepared and annealed nano-TiO_2 with the fitted pattern by Rietveld method along with the difference plot

Low temperature annealing at 100 °C does not produce any significant change in the X-ray diffraction pattern. Annealing at 500 °C reduces the broadening of the peaks but the phase still remains a-TiO_2. Thus, it is clear that the anatase phase is stable upto 500 °C. The progression of broadening suggests that there is a decrease in the strain broadening and hence a relaxation of microstrain is predicted. A considerable change in the diffraction pattern was observed when a higher annealing temperature (~ 750 °C) was selected. A partial anatase to rutile phase transformation along with narrowing of the X-ray diffraction lines was observed. The narrowing of the diffraction pattern can be attributed to grain growth and relaxation of microstrains. It was further observed that even at a temperature of 1000 °C, the transformation of the anatase phase to the rutile phase is not complete. To determine the crystallite size, lattice microstrain, morphology of the crystallites, phase quantification and other structural parameters a detailed structural and microstructural characterization was undertaken on the basis of modified Rietveld method and is discussed in the subsequent sections.

Rietveld analysis

To perform microstructural analysis using modified Rietveld method, it is essential to simulate the initial diffraction pattern. The Rietveld program MAUD [46] was used for the purpose of simultaneous structure and microstructure refinement. Since there were no other impurity phases present in the samples, structural coordinates of only a-TiO_2 and r-TiO_2 were used for the purpose of pattern simulation and subsequent refinement.

In the program MAUD, the effect of the microstructural features like crystallite size and microstrain on the line broadening is obtained by approximating the diffraction line shapes by pseudo-Voigt analytical functions. A pseudo-Voigt function is a linear combination of a Gauss and Lorentz functions and is mathematically given by the expression

$$pV(x) = \eta L(x) + (1 - \eta)G(x), \tag{1}$$

where η is known as the mixing parameter representing the Lorentzian fraction.

The integral breadth of a pseudo-Voigt function is expressed as

$$\beta = \omega\left[\pi\eta + (1 - \eta)(\pi/\ln 2)\right], \tag{2}$$

where w is the half width at half maxima.

The volume-weighted crystallite size (D) and maximum microstrain (e) are obtained according to the following relations:

$$D = {}^{\lambda}/_{\beta_c^f \cos\theta}, \tag{3}$$

$$e = {}^{\beta_G^f}/_{4\tan\theta}, \tag{4}$$

where β^f represents the true specimen broadened profile and the subscripts C and G corresponds to lorentzian and the Gaussian components, respectively.

The method of whole pattern fitting/ Rietveld method adopted by us is essential for the analysis of XRD pattern of as-synthesised TiO_2 due to its complexity and presence of multiple phases. Methods based on peak fitting to determine the peak width/profile shape parameters and the subsequent use of Williamson–Hall or other variants produces inaccurate results in size / strain due to extensive peak overlap. The refinement protocol performed in our case was a two-step one. In the first step lattice parameter, microstructural parameters and the phase fractions were refined and second, the structural parameters were refined. In the program MAUD, the crystallite size and the microstrain is held as a refinable parameter. The microstructural model used refinement is an isotropic size–strain model. The adopted model yields the value of volume-weighted crystallite size and maximum value of lattice microstrain.

Figure 1 shows the fitted diffraction pattern along with the difference plot and Table 1 lists the results of Rietveld refinement. The goodness-of-fit (*Gof*) varies between 1.15 and 1.28 for the samples analysed. Anisotropic size–strain model did not improve the goodness-of-fit, indicating that the particles are nearly isotropic in shape, which is in agreement with TEM studies. Table 1 also lists the values of crystallite size and microstrains.

Figure 2 shows the plot of the refined lattice parameters 'a' and 'c' for the a-TiO_2 phase with the annealing temperature. It is found in the plot that the lattice parameter 'a' is slightly larger than the equilibrium value, whereas the other lattice parameter 'c' is slightly smaller than the equilibrium value. Annealing at temperature above 750^0C yields the equilibrium value of the lattice parameters. The unit cell volume is approximately ~ 137 $Å^3$ for the a-TiO_2 in the nanocrystalline state. For the a-TiO_2 phase, the evolution of the unit-cell parameters with the annealing temperature is the same for all the samples in accordance with earlier

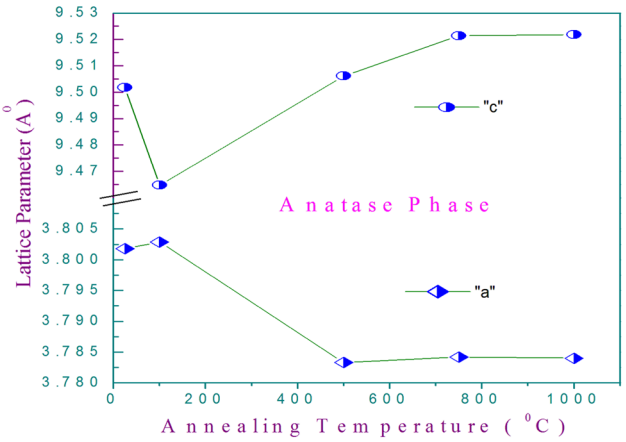

Fig. 2 Variation of lattice parameters of the anatase phase of nano-TiO_2 as a function of the annealing temperature

Table 1 Results from Rietveld analysis for the as-prepared and annealed nanocrystalline TiO_2

	As prepared	Annealed 100 ° C	Annealed 500 ° C	Annealed 750 ° C		Annealed 1000 ° C	
	Anatase	Anatase	Anatase	Anatase	Rutile	Anatase	Rutile
Relative Wt%	1.0	1.0	1.0	48.3	51.7 (5)	45.2	54.8 (3)
Cell (Å)							
a	3.801 (1)	3.803 (1)	3.783 (02)	3.784 (0.07)	4.594 (0.05)	3.784 (0.07)	4.594 (0.04)
c	9.502 (5)	9.465 (5)	9.506 (0.7)	9.521 (0.3)	2.960 (0.06)	9.522 (0.3)	2.960 (0.05)
Size (nm)	3.0 (0.04)	3.0 (0.07)	9.0 (0.08)	60.0 (1.0)	122.0 (3.0)	62.0 (1.0)	125.0 (2.0)
Strain ($\times 10^2$)	1.550 (4)	1.690 (9)	0.590 (8)	0.157 (5)	0.035 (6)	0.161 (7)	0.038 (5)
O_x	0.0	0.0	0.0	0.0	0.3058 (4)	0.0	0.3049 (4)
O_y	0.0	0.0	0.0	0.0	0.3058 (equal)	0.0	0.3049 (equal)
O_z	0.212 (0.5)	0.213 (0.5)	0.207 (0.6)	0.207 (0.8)	0.0	0.207 (0.7)	0.0
$B_{\text{iso Ti}}$	2.33 (18)	2.47 (23)	0.64 (4)	0.55 (5)	0.77 (4)	0.52 (5)	0.74 (4)
$B_{\text{iso O}}$	0.0 (fix)	0.0 (fix)	1.45 (9)	1.18 (5)	0.79 (4)	1.26 (9)	0.84 (8)
R_{wp}	5.548	5.696	6.438	6.317		6.678	
R_b	4.425	4.571	5.063	4.874		5.165	
Gof	1.150	1.161	1.282	1.224		1.194	

studies [33, 34]. Swami et. al [34] observed similar behavior for nanocrystallite of size below 10 nm. However, there is a small lattice contraction for samples annealed at 100° C, in our case, is in clear distinction from earlier result [34]. It is further clear from Fig. 2 that the variation of the lattice parameter is highly non-linear with increasing temperature in broad agreement with earlier studies and proves that the this behavior is universal for sol–gel derived samples (egs. Ref. [33] and [34]). Some authors observed Ti vacancy for samples below the size limit of 10 nm [34]. However, varying the Ti vacancy parameter did not improve our *Gof* values and we did not observe any Ti vacancy in the **as synthesized or annealed** nanocrystalline anatase phase unlike as in [34]. On the contrary, a change in the thermal parameter was observed in our case (see below) which indicates static disorder probably in the crystallite boundaries.

It is further observed from Table 1 that upto an annealing temperature of 500 °C, there is no anatase to rutile phase transformation. However, when the annealing temperature was raised to 750 °C there was a drastic change in the phase fraction. The phase fraction didn't undergo any further change after annealing at 1000 °C The maximum phase fraction of the rutile phase observed in the present study is ~ 55% at 1000 °C. It is well known that for TiO_2, the anatase to rutile phase transformation takes place between 500–900 °C [12, 38, 47–51] and the transition temperature is a sensitive function of sample preparation technique. In pure anatase, as in our case, rutile phase may have nucleated at the {112} twin interfaces of two anatase particles. The observed anatase to rutile transformation is reconstructive in nature during which breaking and reforming of bonds takes place [12]. The anatase to rutile transformation involves a contraction of the c-axis and an overall volume contraction of 8% [12] which explains the lattice contraction observed by us as after annealing at 100° C described in the previous paragraph. The phase transformation is always accompanied by a significant grain growth [51]. Patra et al. [51] concluded that chemically synthesized TiO_2 nanoparticles, the anatase to rutile phase transformation temperature is dependent on crystallite size and for crystallites of sizes of the order of 4 nm and there is a delayed phase transformation at around 850 °C. From the thermodynamical point of view, the rutile phase is the most stable polymorphic form of TiO_2. It is further known that the chemical synthesis processes leads to the formation of metastable anatase phase. This may be due to the contribution of the free surface energy of the lower particle sizes obtained by those methods. A critical size of ~ 14 nm has been proposed theoretically by Zhang and Banfield [52] for anatase to rutile transformation. Figure 3 shows the plot of crystallite size and r.m.s. microstrains obtained from modified Rietveld analysis with the annealing temperature. It was revealed that the as-prepared TiO_2 samples were truly nanocrystalline and the crystallite size is of the order of

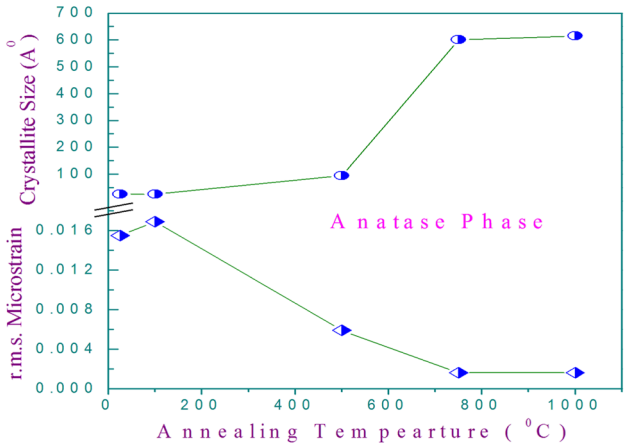

Fig. 3 Variation of crystallite size and the r.m.s. microstrain of the anatase phase of nano-TiO_2 as a function of the annealing temperature

3 nm and a strain level of approximately 1%. Low temperature annealing at 100 °C does not produce any measurable change in either the crystallite size or the microstrain. When the calcination temperature is increased to 500 °C, the crystallite size increases almost threefold (~ 9 nm), but there is a drastic change in the lattice microstrain. Since this crystallite size is less than that of the critical crystallite size, no phase transformation was observed as expected. Annealing at a higher temperature of 750 °C results in drastic grain growth and strain relaxation. The value of anatase crystallite size increased to 60 nm with a concomitant decrease in the lattice micostrain to ~ 0.1% from a value of 0.6%. However, the crystallite size of the rutile phase is approximately twice that of the anatase phase. Further, annealing upto 1000° C did not produce any appreciable change in the values of either the crystallite size/microstrain or phase fraction. It is thus clear that there is a discontinuous change in the size and strain values associated with a concomitant phase change. The value of lattice microstrain in the present study is comparable to that obtained in other studies [11, 30–34] for similar values of crystallite sizes. However, a different trend was observed by Patra et al. [51] who observed that phase transformation is complete when the particles reach a crystallite size of 60 nm. In our case, approximately 45% retention of anatase crystallite in the nano TiO_2 sample is possible by our present synthesis method. Further, they [51] did not consider the effect of microstrain in their analysis, which seems an important parameter during phase transformation.

Table 1 further lists the values of isotropic thermal parameters of the Ti atom and z-displacement of O atom. A similar discontinuous change at 750 °C could be observed. The measured z-displacement parameters of the oxygen atom in the nanocrystalline state is significantly different from the course grained material (the sample annealed at 1000 °C can be considered to be coarse grained). The value

of thermal parameter B indicates that there is a significant deviation of the Ti atom from the regular lattice sites. It must be mentioned here that thermal parameter B consists of two components, B_T and B_S, where B_T is the contribution from thermal vibration and B_S is independent of temperature and implies static lattice distortion. Since the B parameter was not measured at different temperatures, the two contributions could not be separated. But results still indicate that there significant deviation of the Ti atom from the regular lattice sites.

The dependence of the microstructural parameter viz microstrain and the structural parameters viz the thermal parameter B and the z-displacement of the oxygen atom on the crystallite size is shown graphically in Fig. 4. It is clear from the figure that a near hyperbolic dependence is observed in all cases. It may be inferred that the origin of lattice microstrain in the nanocrystalline TiO_2 is the disorder observed in the nanocrystalline state. A one to one correspondence has been observed in the present case.

TEM analysis

To provide further insight into the particle/ crystallite size and shape, the growth of the crystallites during phase transition and the size distribution, high-resolution transmission electron microscopy (HRTEM) images were recorded for both the as-prepared and the annealed samples. Figure 5, 6, 7, 8 shows some selected micrographs. Figure 5 displays the HRTEM micrograph of as-prepared nanocrystalline TiO_2 particles. To obtain the average particle size and hence the distribution of particle sizes, average diameters of about 250 particles were measured from different HRTEM images and a histogram is drawn as shown in the inset of Fig. 5. From the histogram, the average particle

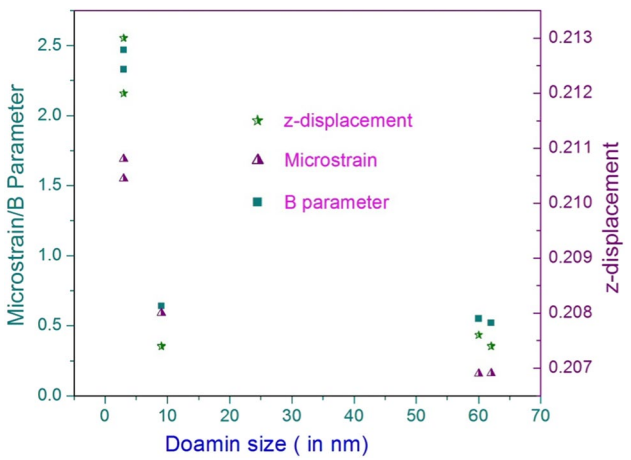

Fig. 4 Variation of the microstrain, the thermal parameter B and the z-displacement of the oxygen atom as a function of the crystallite size for the in the nanocrystalline TiO_2

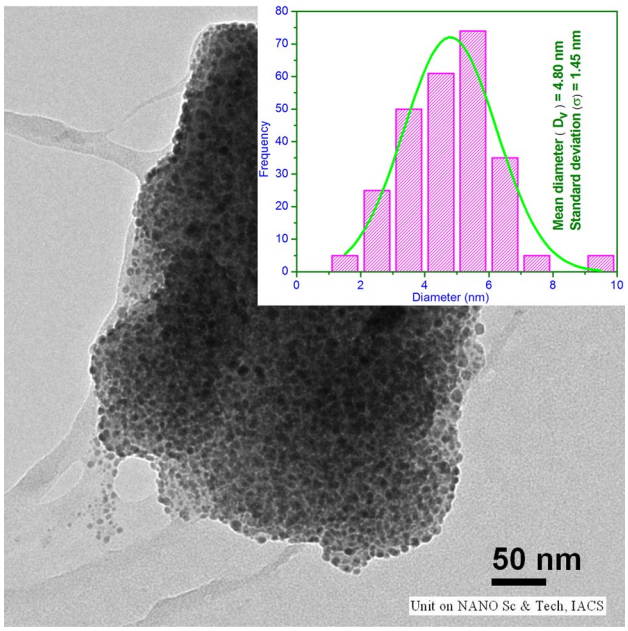

Fig. 5 TEM micrograph of as-prepared nanocrystalline anatase-TiO_2 and (inset) the histogram along with the particle size distribution

diameter obtained is about 5 nm with a standard deviation of 1.4 nm, when fitted with a Gaussian function (solid line). The selected area diffraction pattern (SAED) is also shown in the inset of Fig. 6. From the lattice fringe pattern and the SAED ring in Fig. 6, the measured inter planer spacing is about 3.53 Å, which corresponds to (101) lattice planes of anatase TiO_2. However, we could not detect

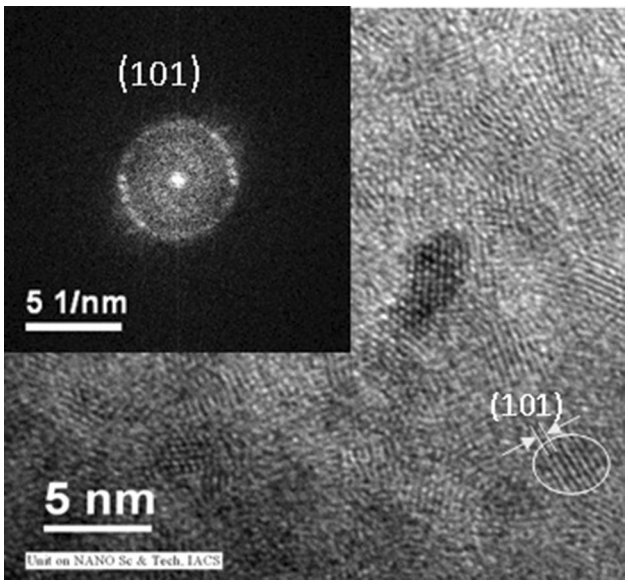

Fig. 6 Single crystallite lattice fringe pattern from HRTEM micrograph of as-prepared nanocrystalline anatase TiO_2 and (inset) the SAED pattern

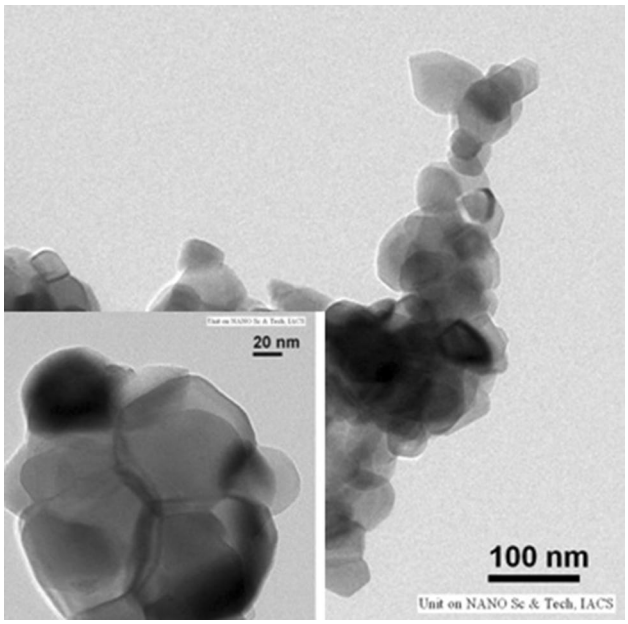

Fig. 7 TEM micrograph of 750 °C annealed nanocrystalline TiO_2 and (inset) the HRTEM image showing the morphology

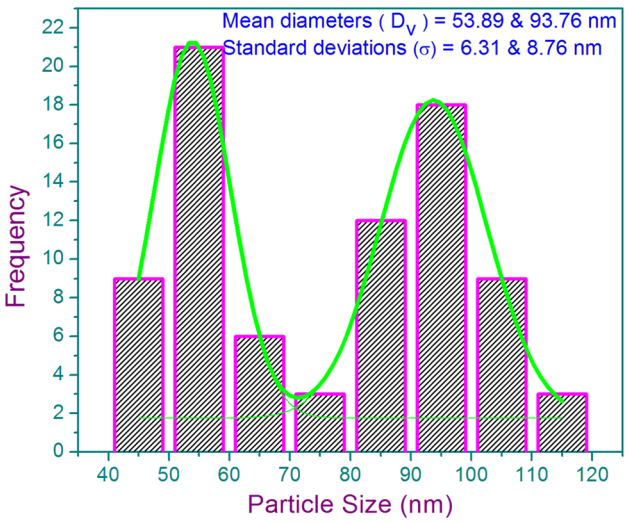

Fig. 8 Histogram along with the particle size distribution obtained from the TEM micrographs of 750 °C annealed nanocrystalline TiO_2

dislocation in the nanocrystalline grains (shown in the encircled region) contrary to that claimed in Ref. [31]. These observations are in agreement with that obtained from the Rietveld analysis of X-ray diffraction pattern, where a crystallite size of 3 nm was observed. It may be mentioned here that the size obtained from X-ray is a volume weighted crystallite size [29]. To compare the X-ray size with that obtained from TEM requires further assumption. For spherical particles, X-ray crystal size should be multiplied with a factor of 4/3. In the present case, X-ray particle size is ~ 4 nm which is in good agreement with the obtained TEM particle size value of 5 nm.

The HRTEM micrographs for the 750 °C annealed sample are shown in Fig. 7. The particle morphology is shown in inset. The distribution of particle size is obtained from the histogram as shown in Fig. 8. From the histogram, it is clear that the particles are distributed about two distinctly different diameters. On fitting by two Gaussian function, mean particle sizes obtained are 54 nm (± 6 nm) and 94 nm (± 9 nm). From the X-ray powder diffraction pattern, it has been observed in the earlier section that a phase transformation has occurred at 750^0C with the appearance of rutile TiO_2 phase. Moreover, the Rietveld analysis reveals that the phase transition is accompanied with a radical grain growth. The resulting grain size of the newly formed rutile phase is of the order of approximately 120 nm, almost two times to that of anatase phase. Thus, the observations from HRTEM study for both the as-prepared antase nanocrystalline TiO_2 as well as the annealed samples correspond to the results obtained in the earlier section from X-ray powder diffraction profile analysis.

Conclusion

Nanocrystalline TiO_2 has been prepared by synthetic route. The phase transformation and the microstructural changes of nano-TiO_2 with the annealing temperature have been investigated by modified Rietveld analysis of X-ray powder diffraction profiles and transmission electron microscopy. From the above experimental observations, following conclusions can be drawn. The as-prepared nanocrystalline TiO_2 is found to be in purely anatase phase with a probability of the presence of amorphous phase. A partial anatase to rutile phase transformation has occurred at an annealing temperature of 750^0C. The phase transformation is not complete even at a higher temperature of 1000 °C and an approximately 45% anatase phase can be retained in the nanocrystalline sample. The crystallite size of the retained anatase phase is of the order of 60 nm. The lattice parameter a of the anatase TiO_2 in the nanocrystalline form is larger than its equilibrium value and reverse holds for the other lattice parameter c and it changes non linearly with the annealing temperature. The grain size of the as-prepared anatase TiO_2 is of the order of 3 nm with a significant amount of microstrain (~ 0.016) in broad agreement with the TEM data. Measurement of thermal parameter and absence of dislocations indicate static disorder of the Ti atom which is deviated from the regular lattice sites in the nanocrystalline state and explains the origin of lattice microstrain. The phase transformation is associated with a drastic grain growth, strain relaxation and reduced static disorder.

Author contributions Both the authors have contributed equally in the manuscript.

References

1. Fujishima, A., Zhang, X.: Titanium dioxide photocatalysis: present situation and future approaches. CR Chim. **9**, 750–760 (2006)
2. Hashimoto, K., Irie, H., Fujishima, A.: TiO_2 photocatalysis: a Historical overview and future prospects. Jpn. J. Appl. Phys. **44**, 8269–8285 (2005)
3. Wang, R., Hashimoto, K., Fijishima, A., Chikuni, M., Kojima, E., Kitamura, A., Shimohigoshi, M., Watanabe, T.: Light-induced amphiphilic surfaces. Nature **388**, 431–432 (1997)
4. Sakai, N., Fujishima, A., Watanabe, T., Hashimoto, K.: Quantitative evaluation of the photoinduced hydrophilic conversion properties of TiO_2 thin film surfaces by the reciprocal of contact angle. J. Phys. Chem. B. **107**, 1028–1035 (2003)
5. Mills, A., Hill, G., Bhopal, S., Parkin, I.P., O'Neill, S.A.: Thick titanium dioxide films for semiconductor photocatalysis. J. Photochem. Photobiol. A **160**, 185–194 (2003)
6. Sopyan, I., Watanabe, M., Murasawa, S., Hashimoto, K., Fujishima, A.: An efficient TiO_2 thin-film photocatalyst: photocatalytic properties in gas-phase acetaldehyde degradation. J. Photochem. Photobiol. A **98**, 79–86 (1996)
7. Matsunaga, T., Tomoda, R., Nakajima, T., Wake, H.: Photoelectrochemical sterilization of microbial cells by semiconductor powders. FEMS Microbiol. Lett. **29**, 211–214 (1985)
8. Evans, P., Sheel, D.W.: Photoactive and antibacterial TiO_2 thin films on stainless steel. Surf. Coat Technol. **201**, 9319–9324 (2007)
9. Hart, J.N., Cervini, R., Cheng, Y.B., Simon, G.P., Spiccia, L.: Formation of anatase TiO_2 by microwave processing. Sol. Energy Mater. Sol. Cells. **84**, 135–143 (2004)
10. Ni, M., Leung, M.K.H., Leung, D.Y.C., Sumathy, K.: A review and recent developments in photocatalytic water-splitting using $TiO_2$for hydrogen production. Ren. Sust. Energy Rev. **11**, 401–425 (2007)
11. Dam, T., Jena, S.S., Pradhan, D.K.: Equilibrium state of anatase to rutile transformation of nano-structured titanium dioxide powder using polymer template method. IOP Conf. Ser. Mater. Sci. Eng. **115**, 0120381–0120386 (2016)
12. Hanao, D.A.H., Sorrell, C.C.: Review of the anatase to rutile phase transformation. J. Mater. Sci. **46**, 855–874 (2011)
13. Vasquez, G.C., Peche-Herrero, M.A., Maestre, D., Gianoncelli, A., Ramirez-Castellanos, J., Cremades, A., Gonzalez-Calbet, J.M., Piqueras, J.: Laser-induced anatase-to-rutile transition in TiO_2 nanoparticles: promotion and inhibition effects by Fe and Al doping and achievement of micropatterning. J. Phys. Chem. C **119**, 11965–11974 (2015)
14. Bhatkhande, D.S., Pangarkar, V.G., Beenackers, A.: Photocatalytic degradation for environmental applications: a review. J. Chem. Technol. Biotechnol. **77**, 102–116 (2001)
15. Sarah, S.W., Donia, B., Scott, J.A., Amal, R.: The effect of preparation method on the photoactivity of crystalline titanium dioxide particles. Chem. Eng. J. **95**, 213–220 (2003)
16. Fotou, G.P., Vemury, S., Pratsinis, S.E.: Synthesis and evaluation of titania powders for photodestruction of phenol. Chem. Eng. Sci. **49**, 4939–4948 (1994)
17. Chou, T.C., Ling, T.R., Yang, M.C., Liu, C.C.: Micro and nano scale metal oxide hollow particles produced by spray precipitation in a liquid–liquid system. Mater. Sci. Eng. A **359**, 24–30 (2003)
18. Yamabi, S., Imai, H.: Synthesis of rutile and anatase films with high surface areas in aqueous solutions containing urea. Thin Solid Films **434**, 86–93 (2003)
19. Obuchi, E., Sakamoto, T., Nakano, K., Shiraishi, F.: Photocatalytic decomposition of acetaldehyde over TiO_2/SiO_2 catalyst. Chem. Eng. Sci. **54**, 1525–1530 (1999)
20. Yamashita, H., Harada, M., Misaka, J., Takeuchi, M., Ikeue, K., Anpo, M.: Degradation of propanol diluted in water under visible light irradiation using metal ion-implanted titanium dioxide photocatalysts. J. Photochem. Photobiol. A **148**, 257–261 (2002)
21. Zimbone, M., Buccheri, M.A., Cacciato, G., Sanz, R., Rappazzo, G., Boninelli, S., Reitano, R., Romano, L., Privitera, V., Grimaldi, M.G.: Photocatalytical and antibacterial activity of TiO_2 nanoparticlesobtained by laser ablation in water. Appl. Catal. B **165**, 487–494 (2015)
22. Liu, P., Cai, W., Fang, M., Li, Z., Zeng, H., Hu, J., Luo, X., Jing, W.: Room temperature synthesized rutile TiO_2 nanoparticles induced by laser ablation in liquid and their photocatalytic activity. Nanotechnology **20**, 2857071 (2009)
23. Barreca, F., Acacia, N., Barletta, E., Spadaro, D., Curro, G., Neri, F.: Small size TiO_2 nanoparticles prepared by laser ablation in water. Appl. Surf. Sci. **256**, 6408–6412 (2010)
24. Wu, S., Weng, Z., Liu, X., Yeung, K.W.K., Chu, P.K.: Functionalized TiO_2 based nanomaterials for biomedical applications. Adv. Funct. Mater. **24**, 5464–5481 (2014)
25. Chen, X., Mao, S.S.: Titanium dioxide nanomaterials: synthesis, properties, modifications, and applications. Chem. Rev. **107**, 2891–2959 (2007)
26. Arimitsu, N., Nakajima, A., Saito, K., Kameshima, Y., Okada, K.: Effects of vacuum ultraviolet light illumination on the residual stress in sol–gel-derived titanium dioxide films. Chem. Lett. **36**, 106–107 (2007)
27. Choudhury, B., Choudhury, A.: Local structure modification and phase transformation of TiO_2 nanoparticles initiated by oxygen defects, grain size, and annealing temperature. Int. Nano Lett. **3**, 55–63 (2013)
28. Tripathi, A.K., Singh, M.K., Mathpal, M.C., Mishra, S.K., Agarwal, A.: Study of structural transformation in TiO_2 nanoparticles and its optical properties. J. Alloys Compd. **549**, 114–120 (2013)
29. Cullity, B.D., Stock, S.R.: Elements of X-Ray Diffraction. Pearson, Harlow (2013)
30. Chenari, H.M., Seibel, C., Hauschild, D., Reinert, F., Abdollahian, H.: Titanium dioxide nanoparticles: synthesis, x-ray line analysis and chemical composition study. Mater. Res. **19**, 1319–1323 (2016)
31. Rajender, G., Giri, P.K.: Strain induced phase formation, microstructural evolution and bandgap narrowing in strained TiO_2 nanocrystals grown by ball milling. J. Alloys Compd. **676**, 591–600 (2016)
32. Seetharaman, A., Dhanuskodi, S.: Micro-structural, linear and nonlinear optical properties of titania nanoparticles. Spectrochim. Acta Part A **127**, 543–549 (2014)
33. Vives, S., Meunier, C.: Influence of the X-ray diffraction line profile analysis method on the structural and microstructural parameters determination of sol-gel TiO_2 powders. Powder Diffr. **24**, 205–220 (2009)
34. Swamy, V., Menzies, D., Muddle, B.C., Kuznetsov, A., Dubrovinsky, L.S., Dai, Q., Dmitriev, V.: Nonlinear size dependence of anatase TiO_2 lattice parameters. Appl. Phys. Lett. **88**, 2431031 (2006)
35. Edelson, L.H., Glaeser, A.M.: Role of particle substructure in the sintering of monosized titania. J. Am. Ceram. Soc. **71**, 225–235 (1988)
36. Kumar, K.N.P., Keizer, K., Burggraaf, A.J.: Stabilization of the porous texture of nanostructured titanic by avoiding a phase transformation. J. Mat. Sci. Lett. **13**, 59–61 (1997)
37. Barsoum, M.W.: Fundamentals of Ceramics. Mc-Graw Hill, New York (1997)

38. Bahnemann, D.W.: Ultrasmall metal oxide particles: preparation, photophysical characterization, and photocatalytic properties. Isr. J. Chem. **33**, 115–136 (1993)
39. Colombo, D.P., Roussel, K.A., Saeh, J., Skinner, D.E., Cavaleri, J.J., Bowman, R.M.: Femtosecond study of the intensity dependence of electron-hole dynamics in TiO_2 nanoclusters. Chem. Phys. Lett. **232**, 207–214 (1995)
40. van Berkum, J.G.M., Sprong, G.J.M., de Keijser, ThH, Delhez, R., Sonneveld, E.J.: The optimum standard specimen for X-ray diffraction line-profile analysis. Powder Diffr. **10**, 129–139 (1995)
41. Hanaor, D.A.H., Assadi, M.H.N., Li, S., Yu, A., Sorrell, C.C.: Ab initio study of phase stability in doped TiO_2. Comput. Mech. **50**, 185–194 (2012)
42. Bakardjieva, S., Subrt, J., Stengl, V., Dianez, M.J., Sayagues, M.J.: Photoactivity of anatase–rutile TiO_2 nanocrystalline mixtures obtained by heat treatment of homogeneously precipitated anatase. Appl. Catal. B **58**, 193–202 (2005)
43. Ohno, T., Sarukawa, K., Matsumura, M.: Crystal faces of rutile and anatase TiO_2 particles and their roles in photocatalytic reactions. New J. Chem. **26**, 1167–1170 (2002)
44. Testino, A., Bellobono, I.R., Buscaglia, V., Canevali, C., D'Arienzo, M., Polizzi, S., Scotti, R., Morazzoni, F.: Optimizing the photocatalytic properties of hydrothermal TiO_2 by the control of phase composition and particle morphology. A systematic approach. J. Am. Chem. Soc. **129**, 3564–3575 (2007)
45. Ohtani, B., Handa, J., Nishimoto, S., Kagiya, T.: Highly active semiconductor photocatalyst: Extra-fine crystallite of brookite TiO_2 for redox reaction in aqueous propan-2-ol and/or silver sulfate solution. Chem. Phys. Lett. **120**, 292–294 (1985)
46. Lutterotti, L., Matthies, S., Wenk, H.R.: MAUD: a friendly Java program for Material Analysis Using Diffraction. IUCR Newsl. CPD **21**, 14–15 (1999)
47. Czanderna, A.W., Rao, C.N.R., Honig, J.M.: The anatase-rutile transition. Part 1-kinetics of the transformation of pure anatase. Trans. Faraday Soc. **54**, 1069–1073 (1958)
48. Hague, D.C., Mayo, M.J.: Controlling crystallinity during processing of nanocrystalline titania. J. Am. Ceram. Soc. **77**, 1957–1960 (1994)
49. Haro-Poniatowski, E., Rodriguez-Talavera, R., Heredia, M.D.C., Cano-Corona, O., Arroyo-Murillo, R.: Crystallization of nanosized titania particles prepared by the sol-gel Process. J. Mater. Res. **9**, 2102–2108 (1994)
50. Sheinkman, A.I., Tymentsev, V.A., Fotiev, A.A.: Titanium dioxide recrystallization stimulated by phase transition. Izv. Akad. Nauk SSSR Neorg. Mater. **20**, 1692–1694 (1984)
51. Patra, S., Davoisne, C., Bouyanfif, H., Foix, D., Sauvage, F.: Phase stability frustration on ultrananosized anatase TiO2. Sci Rep **5**, 10928 (2015)
52. Zhang, H., Banfield, J.F.: Thermodynamic analysis of phase stability of nanocrystalline titania. J. Mater. Chem. **8**, 2073–2076 (1998)